Intracellular targets of cyclin-dependent kinase inhibitors: identification by affinity chromatography using immobilised inhibitors

M Knockaert[1], N Gray[2], E Damiens[1], Y-T Chang[3], P Grellier[4], K Grant[5], D Fergusson[5], J Mottram[5], M Soete[6], J-F Dubremetz[6], K Le Roch[7], C Doerig[7], PG Schultz[2] and L Meijer[1]

Background: Chemical inhibitors of cyclin-dependent kinases (CDKs) have great therapeutic potential against various proliferative and neurodegenerative disorders. Olomoucine, a 2,6,9-trisubstituted purine, has been optimized for activity against CDK1/cyclin B by combinatorial and medicinal chemistry efforts to yield the purvalanol inhibitors. Although many studies support the action of purvalanols against CDKs, the actual intracellular targets of 2,6,9-trisubstituted purines remain unverified.

Results: To address this issue, purvalanol B (**95**) and an N6-methylated, CDK-inactive derivative (**95M**) were immobilized on an agarose matrix. Extracts from a diverse collection of cell types and organisms were screened for proteins binding purvalanol B. In addition to validating CDKs as intracellular targets, a variety of unexpected protein kinases were recovered from the **95** matrix. Casein kinase 1 (CK1) was identified as a principal **95** matrix binding protein in *Plasmodium falciparum*, *Leishmania mexicana*, *Toxoplasma gondii* and *Trypanosoma cruzi*. Purvalanol compounds also inhibit the proliferation of these parasites, suggesting that CK1 is a valuable target for further screening with 2,6,9-trisubstituted purine libraries.

Conclusions: That a simple batchwise affinity chromatography approach using two purine derivatives facilitated isolation of a small set of highly purified kinases suggests that this could be a general method for identifying intracellular targets relevant to a particular class of ligands. This method allows a close correlation to be established between the pattern of proteins bound to a small family of related compounds and the pattern of cellular responses to these compounds.

Addresses: [1]Station Biologique de Roscoff, CNRS, BP 74, 29682 Roscoff cedex, Bretagne, France. [2]Novartis Institute for Functional Genomics, 3115 Merryfield Row, Suite 200, San Diego, CA 92121, USA. [3]The Scripps Research Institute, Department of Chemistry, 10550 N. Torrey Pines Road, La Jolla, CA 92037, USA. [4]Museum d'Histoire Naturelle, EP CNRS 1790, Biologie et Evolution des Parasites, 61 rue Buffon, 75005 Paris, France. [5]Wellcome Centre for Molecular Parasitology, The Anderson College, University of Glasgow, Glasgow G11 6NU, Scotland, UK. [6]Institut de Biologie, Institut Pasteur, 1 rue du Professeur Calmette, 59019 Lille cedex, France. [7]Unité INSERM U511, La Pitié-Salpétrière, 91 Bd de l'Hôpital, 75643 Paris cedex 13, France.

Correspondence: L Meijer
E-mail: meijer@sb-roscoff.fr

Key words: casein kinase 1, cyclin-dependent kinases, erk, malaria, purine

Received: **1 December 1999**
Revisions requested: **5 January 2000**
Revisions received: **15 February 2000**
Accepted: **17 March 2000**

Published: **30 May 2000**

Chemistry & Biology 2000, **7**:411–422

1074-5521/00/$ – see front matter

Introduction

Cyclin-dependent kinases (CDKs) are active as complexes comprising a catalytic subunit and a regulatory subunit (cyclin). Nine CDK proteins and eleven cyclins have been identified in man at present: CDK1 (associated with cyclin B), CDK2 (cyclin A, cyclin E), CDK3 (no associated cyclin identified as yet), CDK4 (cyclin D1–D3), CDK5 (associated with noncyclin proteins, $p35^{nck5a}$ or p39), CDK6 (cyclin D1–D3), CDK7 (cyclin H), CDK8 (cyclin C) and CDK9 (cyclin K, cyclin T). The CDKs associated with cyclins F, G and I have not been identified as yet. CDKs play a key role in cell-cycle control (CDKs 1–4, 6, 7), in thymocyte apoptosis (CDK2), in neuronal functions (CDK5) and in transcription (CDKs 7–9); for reviews see [1–4].

CDKs and their regulators are very frequently deregulated in human tumours. CDK5 is also clearly important in neurodegenerative disorders such as Alzheimer's disease and Parkinson's disease. Stimulated by these observations and by the first encouraging preclinical and clinical results obtained with CDK inhibitors [5,6], the search for chemical inhibitors of CDKs has intensified over the past few years (for reviews see [7–10]). Several potent inhibitors have been described: isopentenyladenine [11], staurosporine [11], butyrolactone I [12], olomoucine [13], flavopiridol [14], roscovitine [15,16], purvalanol [17], indirubins [18], paullones [19,20] and hymenialdisine [21]. All CDK inhibitors identified so far function by competing with ATP for binding to the catalytic site. Many of these inhibitors have been co-crystallised with CDK2 (for a review see [10]). Chemical inhibitors of CDKs may have therapeutic applications in various human diseases such as tumoral proliferation (200 types of cancers), nontumoral proliferation (psoriasis, angiogenesis), cardiovascular diseases (undesired vascular proliferation following angioplasty [restenosis] [22], in arteriosclerosis [23] or atherosclerosis), renal diseases

(glomerulonephritis) [24,25], parasitosis (e.g. proliferation of protozoan organisms [e.g. *Plasmodium*, *Toxoplasma*, *Trypanosoma*] [10], fungi, helminths), viral infections (cytomegalovirus [26], HIV [27], Herpes simplex virus [28], varicella-zoster virus [29]), and neurodegenerative disorders (Alzheimer's disease [21,30,31]).

Since the discovery of 6-dimethylaminopurine [32,33] and isopentenyladenine [11] as inhibitors of CDK1/cyclin B, 2,6,9-trisubstituted purines have been extensively investigated as CDK inhibitors. Following on from classical [13,15,34] or combinatorial chemistry synthesis [35–38], thorough structure–activity relationship studies have been performed, leading to increasingly active purines (for review see [10]): 6-dimethylaminopurine (IC_{50} = 120 μM) [32,33], isopentenyladenine (IC_{50} = 55 μM) [11], olomoucine (IC_{50} = 7 μM) [13], roscovitine (IC_{50} = 0.45 μM) [16], amino-purvalanol (IC_{50} = 0.033 μM; **97**) [39], purvalanol A and B (**60** and **95**; IC_{50} = 0.004–0.006 μM) [17]. As efficiency improved, we noticed a clear increase in kinase selectivity, at least as could be judged from studies performed on a panel of 25–30 kinases. Given the large number of ATP-binding proteins present in cells, the *in vivo* selectivity of CDK inhibitors remains open, thereby limiting interpretations of the cellular effects of CDK inhibitors. Several arguments support the idea that CDK inhibitors act intracellularly by inhibiting CDKs. First, the reported cell-cycle effects are compatible with CDK inhibition (G1 arrest: inhibition of CDK2; G2/M arrest: inhibition of CDK1) (for review see [8]). Second, similar effects are obtained with structurally different inhibitors. Last, a generally good correlation is observed between the *in vitro* efficiency of inhibitors on CDKs, and their *in vivo* efficacy on cells. These arguments are all indirect, however, and the real spectrum of intracellular targets of CDK inhibitors remains unknown.

We therefore designed an affinity-chromatography method to investigate the spectrum of intracellular targets of purine CDK inhibitors. The CDK2–purvalanol crystal structure [10,38] suggested that a linker could be attached to the carboxylic acid of the 6-anilino substituent of the inhibitor without interfering with its interaction with the kinase. This sidechain was used to couple the compound to an agarose matrix. As a control, an inactive N6-methylated purvalanol was also immobilised on agarose. The immobilised purvalanol beads (**95** matrix) were used to affinity purify interacting proteins from various cell types and tissues. A series of very diverse examples demonstrates that purvalanols interact intracellularly with CDKs but also with several other kinases.

Results

Structure and use of affinity chromatography media

An extensive structure–activity relationship study of 2,6,9-trisubstitued purines has led to the discovery of the purvalanols (**95**, **97**; Figure 1), a group of potent and selective CDK inhibitors [17,38]. The crystal structure of purvalanol B (**95**) in the active site of CDK2 shows that the inhibitor nitrogen N6 donates a hydrogen bond to the backbone of Leu83 [17]. Consequently, the addition of a methyl group to N6 (**95M**; **97M**) greatly reduces the CDK inhibitory activity of the compounds [38]. The crystal structure also shows that the 4-carboxyanilino substituent faces the exterior of the kinase, making it ideally suited for modification with a polyethylene glycol linker for coupling to an agarose matrix (Figure 1). The crystal structure also shows that N9 faces the inside of the ATP-binding pocket and is therefore inaccessible to solvent. As another control matrix, **95** was also linked to agarose beads through the N9 position (Figure 1). The **95**, **95M** and **95** N9-linked beads were stored as 33% slurries in bead buffer at 4°C until use. Extracts from various biological models (oocytes, mammalian tissues, protozoan parasites) were loaded on the beads in batch for 30 min, under constant rotation, at 4°C. After extensive washing of the beads, the bound proteins were resolved by 10% sodium dodecyl sulfate–polyacrylamide gel electrophoresis (SDS–PAGE) and analysed either by western blotting, or by silver or Coomassie blue staining. Some protein bands were excised from the gels, digested with endolysine C, and the peptides separated by HPLC and microsequenced. The peptide sequences and identified proteins are shown in Figure 2.

Oocytes and eggs

Starfish oocytes

We first started with one of our favourite cell-cycle models, the starfish oocytes. These cells are naturally arrested in prophase (P) and enter very synchronously into metaphase (M) 20 min after stimulation by the hormone 1-methyladenine [39]. Aminopurvalanol (**97**), but not its methylated derivative (**97M**) (Figure 1), inhibits this prophase/metaphase transition (IC_{50} = 1.8 μM; data not shown). Extracts were prepared from oocytes in prophase or metaphase and loaded on **95**, **95M** and $p9^{CKShs1}$ (a selective CDK1/2-binding protein) beads, and the bound proteins were resolved by electrophoresis and detected by silver staining or western blotting (Figure 3). Besides a major 32 kDa protein that nonspecifically binds to all of the resins, very few proteins interacted with the **95M** matrix. In contrast, several bands bound specifically to the **95** matrix (Figure 3). CDK1 and cyclin B were identified by western blotting (Figure 3b,c). Interestingly, only CDK1/cyclin B from metaphase oocytes bound to the beads, whereas the signal was much reduced on beads loaded with prophase oocytes (compare with the $p9^{CKShs1}$ beads which retain both prophase and metaphase CDK1/cyclin B). This reduced signal probably originates from the small fraction of oocytes that spontaneously mature in the prophase-arrested oocyte population. The lack of binding of prophase CDK1/cyclin B to **95** matrix is probably the consequence of steric hindrance: prophase CDK1

Figure 1

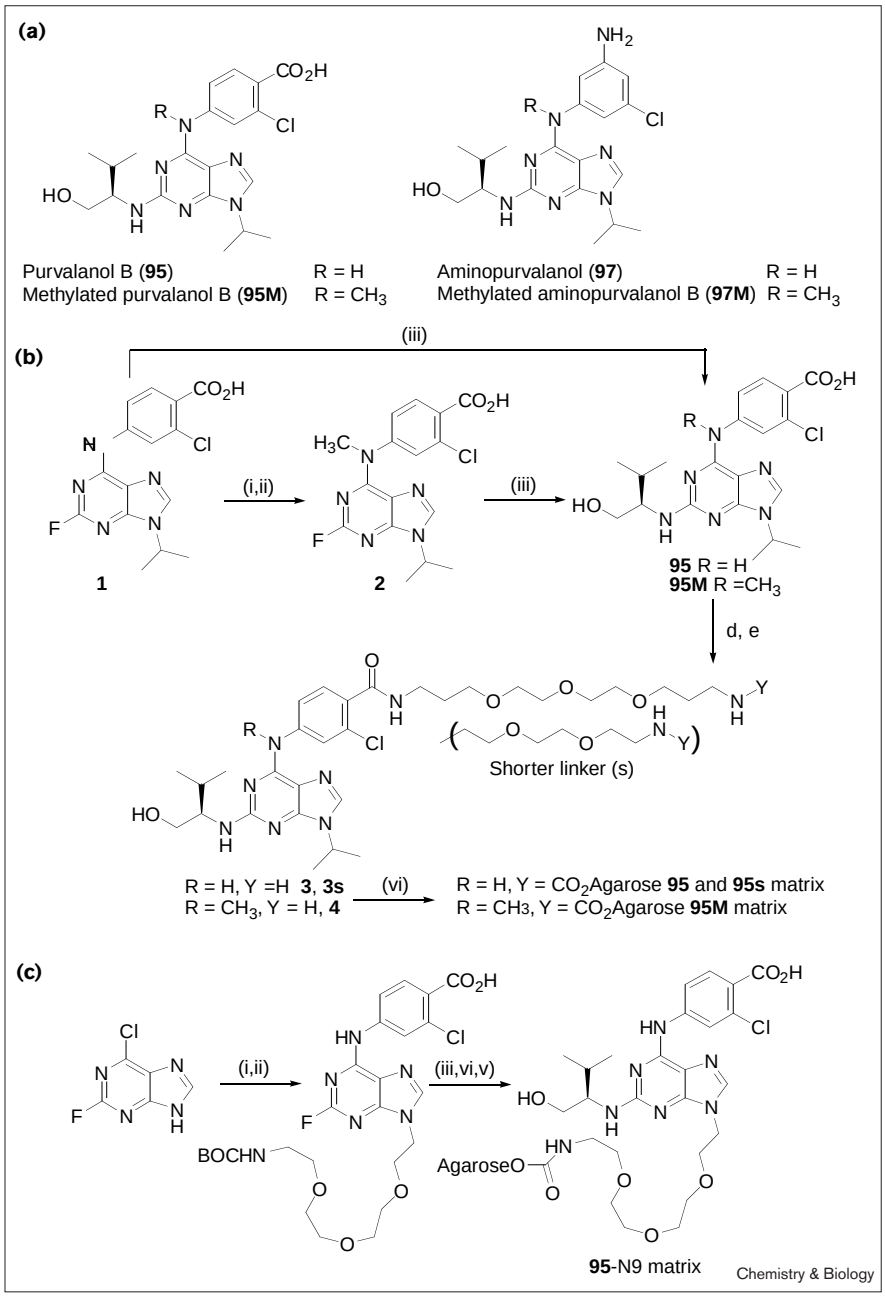

Chemical structures of the purvalanols (**95**, **95M**, **97**, **97M**) and synthetic schemes for the **95**-, **95M**- and **95**-N9 matrices. **(a)** Chemical structures of **95**, **95M**, **97** and **97M**. **(b)** Synthesis of the **95** and **95M** matrices. Conditions: (i) 7.0 equiv. of NaH, 14.0 equiv. of methyliodide, DMF, 12 h; (ii) 1.5 equiv. of NaOH, H_2O/1,4-dioxane (1/1, v/v), 12 h; (iii) 5.0 equiv. of *R*(–)2-amino-3-methyl-1-butanol, 5.0 equiv. of diisopropylethylamine (DIEA), n-butanol, 110°C, 18 h; (iv) 1.05 equiv. of 1,3-diisopropylcarbodiimide (DIC), 1.05 equiv. of hydroxybenzotriazole, 2.0 equiv. of DIEA, 2.0 equiv. of 1-tertbutyloxycarbonyl-1,13-diamino-4,7,10-trioxatridecane, 0.05 equiv. of 4-dimethylaminopyridine, DMF/CH_2Cl_2/1,4-dioxane (1/1/1, v/v/v), 12 h; (v) trifluoroacetic acid/CH_2Cl_2/H_2O/$(CH_3)_2S$ (45/45/1/1, v/v/v/v), 12 h; (vi) 45.0 mM of amine-bearing purine, 1.5 ml of ReactiGel®6× (Pierce, No. 20259), 0.1 M aqueous K_2CO_3, 12 h. **(c)** Synthesis of the **95**-N9 matrix. Conditions: (i) 1.1 equiv. of 13-tertbutoxycarbonylamino-3,6,9-trioxaundecan-1-ol, 2.0 equiv diethylazodicarboxylate, 2.0 equiv. triphenylphosphine, 0°C to RT, 12 h; (ii) 3.0 equiv. of 4-carboxy-3-chloroaniline, 3.0 equiv. of DIEA, n-butanol, 110°C, 12 h; (iii) as (iii) above; (iv) see (v) above; (v) as (vi) above.

is phosphorylated on Thr14 and Tyr15, two sites located at the ATP-binding site, whereas metaphase CDK1 is dephosphorylated at both sites [40]. It has been reported that ATP binds to the doubly phosphorylated CDK1; it is therefore possible that the **95** matrix does not bind the prophase form of CDK1 because the linker cannot be accommodated owing to the presence of the two phosphorylated amino acids that are located just at the border of the ATP-binding site. In addition, we identified two other **95**-binding proteins (Figures 2 and 3a). An 80 kDa protein (**1**), mostly detectable in prophase oocytes, yielded a peptide fragment that displayed homology to a sequence present in ribosomal S6 kinase II. Two peptides resulting from a 53 kDa protein (**2**) shared great homology with calmodulin-dependent kinase II (CaMKII). The presence of both 80 and 53 kDa proteins on the **95** matrix loaded with prophase oocyte extracts, despite the reduced level of CDK1/cyclin B, suggests that these proteins bind directly to the matrix rather than through CDK1/cyclin B. In addition, both proteins did not bind to the $p9^{CKShs1}$ matrix, which strongly binds CDK1. To further confirm this, extracts were depleted of their CDK1/cyclin B on

Figure 2

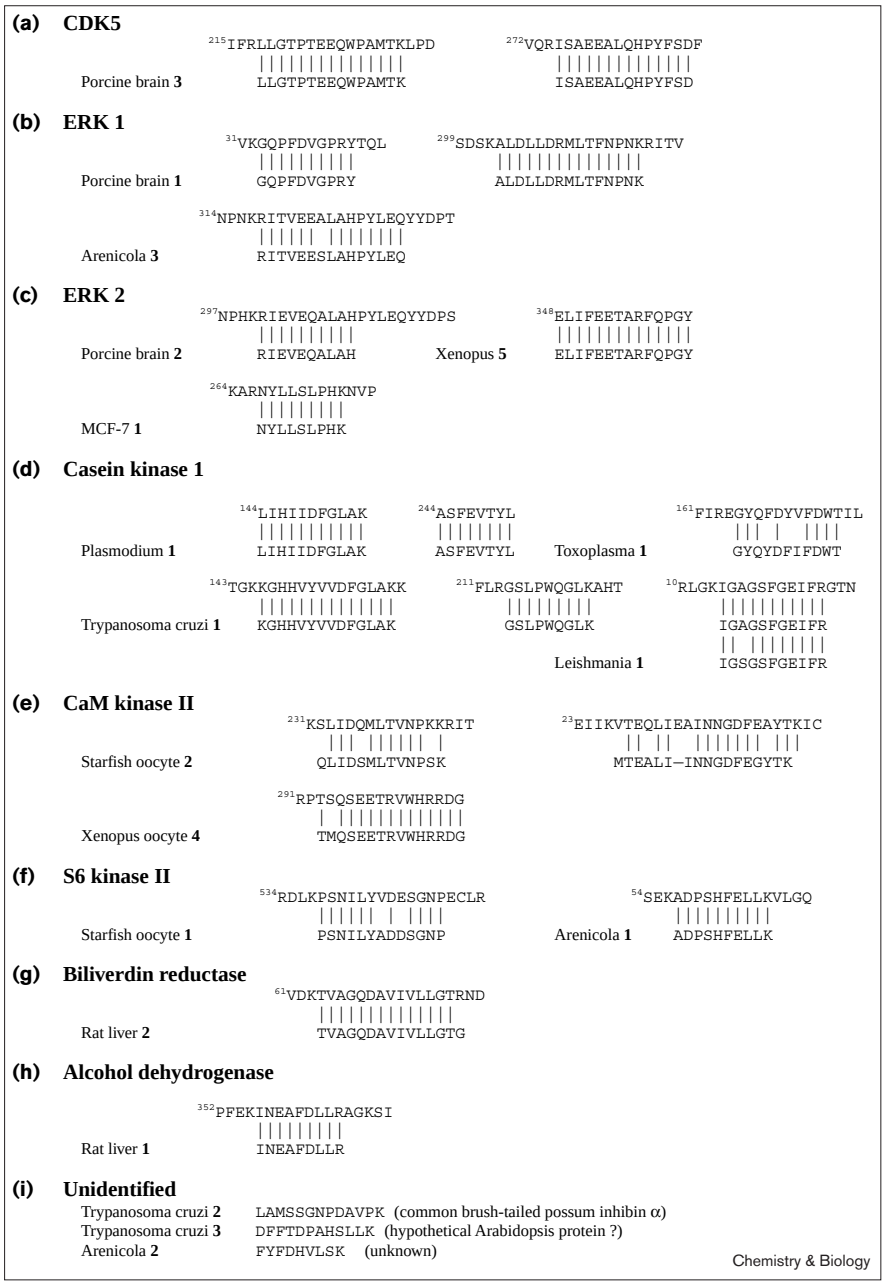

95- and **95M**-binding proteins identified by microsequencing of internal peptides. Proteins were purified from various cell and tissue types by affinity chromatography on **95** and **95M** matrices. Following resolution by SDS–PAGE, individual proteins (numbered for each species as shown in Figures 3–10) were excised from the gel and digested by an endopeptidase. The generated peptides were separated using high performance liquid chromatography (HPLC), and some were microsequenced. Sequences were compared with those present in protein databases. Peptide sequences are presented under a segment of the closest available protein sequence: **(a)** mouse CDK5 (P49615), **(b)** human Erk1 (P27361), **(c)** human Erk2 (Z11694) (porcine brain peptide, MCF-7 peptide), *Xenopus* Erk2 (P26696) (*Xenopus* oocyte peptide), **(d)** *Plasmodium* PfCK1 (AF017139) [44], *T. cruzi* CK1 (AAF-00025) (*Trypanosoma* peptides; *Leishmania* peptide), *Arabidopsis thaliana* CK1 (CAA55397) (*Toxoplasma* peptide), **(e)** rat Ca/calmodulin-dependent kinase II (AAC14706) (first starfish oocyte peptide), *Xenopus* Ca/calmodulin-dependent kinase II (AAA57338) (*Xenopus* oocyte peptide), *Caenorhabditis elegans* Ca/calmodulin-dependent kinase (CAA94244), **(f)** rat S6 kinase II (A53300), **(g)** human biliverdin reductase (NP-000704), **(h)** rat alcohol dehydrogenase (A26468), **(i)** common brush-tailed possum inhibin α subunit (AAC63945), hypohetical *Arabidopsis thaliana* protein (AAD14450).

$p9^{CKShs1}$ beads, before loading on **95** matrix (Figure 4). This depletion did not decrease the levels of proteins **1** and **2**, suggesting that their interactions with **95** matrix is independent of CDK1/cyclin B.

Lugworm oocytes

We then used another marine invertebrate model, the lugworm *Arenicola defodiens*. Its oocytes are also naturally arrested in prophase until stimulated by a brain hormone. After stimulation, they progress into metaphase within 30 min where they remain arrested until fertilisation [41]. We loaded oocyte extracts on **95** and **95M** matrices. Three principal proteins (78, 56, 47 kDa) were found to bind specifically to **95** matrix (Figure 5a). Consistent with the results obtained from the starfish experiments, proteins **1** and **3** were identified as ribosomal S6 kinase II and Erk1, respectively (Figure 2). Peptides derived from protein **2** could not be matched to any known protein sequence, which suggests that this protein might be a novel purine target. In addition, both CDK1 and cyclin B were detected on **95** matrix by western blotting (data not shown).

Figure 3

CDK1/cyclin B and two other proteins from starfish oocytes bind to **95** matrix. Extracts from starfish prophase (P) and metaphase (M) oocytes were loaded on **95M** or **95** matrix, or $p9^{CKShs1}$-sepharose. Bound proteins were resolved by SDS–PAGE and revealed by **(a)** silver staining and by western blotting with **(b)** anti-cyclin B and **(c)** anti-PSTAIRE antibodies. Proteins **1** and **2** were further processed for microsequencing and identified as S6 kinase II and calmodulin-dependent kinase II, respectively (Figure 2).

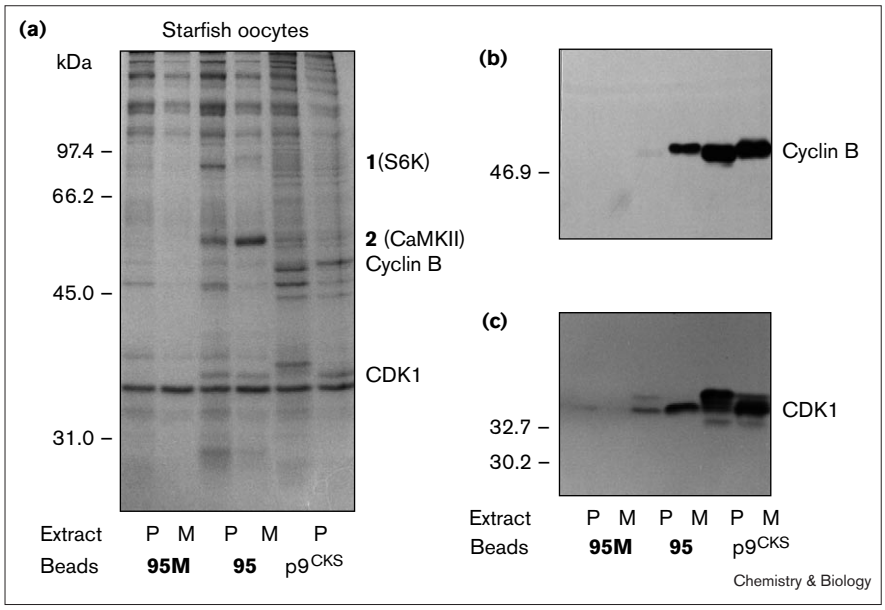

Sea urchin eggs

We then analysed sea urchin eggs, which have been frequently used in cell-cycle studies. These cells are naturally arrested in G1 until fertilisation triggers a series of highly synchronous cell cycles [42]. Extracts were prepared from unfertilised or metaphase eggs and incubated with **95** and **95M** matrices. Two major proteins (32 and 33 kDa) bound specifically to **95** matrix (Figure 5b). The upper band cross-reacts strongly with anti-PSTAIRE antibodies (Figure 5b) and might be either CDK1 or CDK2. The nature of the lower band remains to be determined.

Xenopus *oocytes*

Xenopus laevis oocytes undergo maturation when stimulated by progesterone. Some aspects of this transition can be reproduced in cell-free extracts and they are inhibited by **95** and **97** [43]. We prepared extracts from prophase-arrested oocytes and from oocytes at the time of nuclear-envelope breakdown (GVBD, germinal vesicle breakdown), and loaded them on both matrices. Very few proteins were detected on **95M** (Figure 6a). A few proteins specifically bound to **95** (84, 74, 62, 52, 45 and 33 kDa). Protein **5** was identified as *X. laevis* Erk2, protein **4** as CaMKII, and protein **6** remained an unresolvable mixture (Figure 2). Western blotting allowed the detection of CDK1/CDK2 (anti-PSTAIRE antibodies) and of Erk2 on **95** matrix, but not on **95M** matrix (Figure 6b). As in the starfish oocytes, CDK was only found in matured oocytes, presumably because of the Thr14, Tyr15 phosphorylation of CDKs in prophase oocytes, which is likely to hinder interaction with **95** matrix. Erk2 is inactive in prophase-arrested oocytes and becomes activated during progesterone-induced maturation. This activation by dual phosphorylation of the TEY amino-acid motif is accompanied by a shift in electrophoretic mobility of the kinase. Erk2 was detected in both prophase and matured oocytes (Figure 6b). Using slightly modified electrophoresis conditions, we showed that the **95** matrix binds both the inactive and active forms of Erk2 (Figure 6c).

Mammalian tissues and cells

Rat tissues

Extracts were prepared from various tissues of a male rat and loaded on **95** and **95M** derivatized agarose. No bound proteins were detected on **95M** matrix by silver staining (data not shown), except when loaded with a liver extract which provided an abundant protein (Figure 7, first lane). This 47 kDa protein (**1**) was identified as alcohol dehydrogenase (Figure 2). It was essentially absent on **95** matrix loaded with liver extracts, demonstrating the impressive degree of selectivity achievable by this method. All tissues contained **95**-binding proteins, some of which seemed to be shared by most tissues (such as a 42 kDa protein), others appearing to be tissue-specific (Figure 7). The liver contained a major 26 kDa **95**-interacting protein, which was identified as biliverdin reductase by microsequencing (Figure 2). We are currently investigating the identity of the **95** matrix binding proteins of some of these tissues.

Porcine brain

We then prepared an extract of porcine brain and loaded it on **95** and **95M** matrices. Although essentially no protein was detected on **95M** matrix, three conspicuous proteins (**1**, **2**, **3**) bound specifically to **95** (46, 42, 35 kDa; Figure 8a). They were identified as Erk1, Erk2 and CDK5, respectively (Figure 2). Western blotting showed

Figure 4

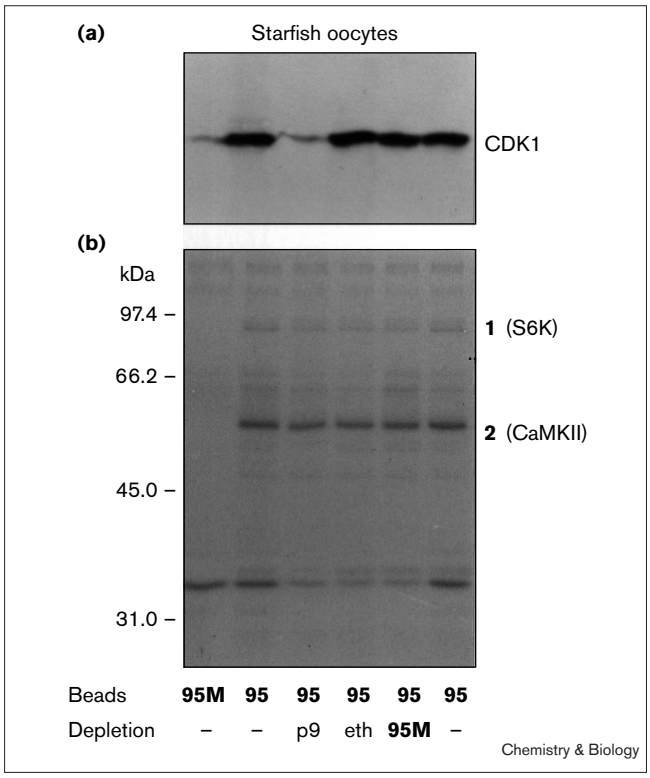

Binding of proteins **1** and **2** is independent of CDK1/cyclin B. Extracts from starfish oocytes were depleted on $p9^{CKShs1}$-sepharose (p9), on control ethanolamine-sepharose beads (eth) or on **95M** matrix before loading on **95** matrix. Bound proteins were resolved by SDS–PAGE and visualised **(a)** by western blotting with anti-PSTAIRE antibodies and **(b)** by silver staining. CDK1 is visualised by the anti-PSTAIRE cross-reactivity.

that p35, the CDK5 activator, and p25, its proteolytic cleavage product, are present (but barely detectable by silver staining) on **95** matrix loaded with brain extracts. There is apparently much more CDK5 than p35/p25, in other words, there is a dominant level of monomeric CDK5 (data not shown). Erk1, Erk2 and CDK5 did not bind to **95** when immobilised through the N9 position (**95N9**; Figure 8b), consistent with an orientation of the inhibitor similar to that observed in the CDK2–purvalanol B crystal structure. All three proteins bound to **95** immobilised through the aniline substituent, even when the sidechain was shortened by five atoms (**95s**; Figures 1 and 8b). As an additional control experiment, we added increasing amounts of ATP to the brain extracts before incubation with **95** matrix. This led to a gradual decrease of CDK5 and Erk1/2 binding to the matrix, confirming the true competitive ATP-binding nature of the interaction with the matrix (data not shown). Similarly addition of increasing levels of free **95** lead to a decreasing binding of the kinases to the **95** matrix (data not shown).

Human cell lines

Extracts prepared from exponentially growing MCF-7 cells were loaded on **95** and **95M** matrices. One principal protein was found to bind specifically to **95** matrix (Figure 9, left). Microsequencing of an internal peptide revealed its identity to be Erk2 (Figure 2), which was further confirmed by western blotting with anti-Erk2 antibodies (Figure 9, right). This binding of Erk2 was confirmed in several other cell lines (data not shown).

Protozoan parasites

Preliminary experiments have shown that purvalanol-derived compounds inhibit the proliferation of several

Figure 5

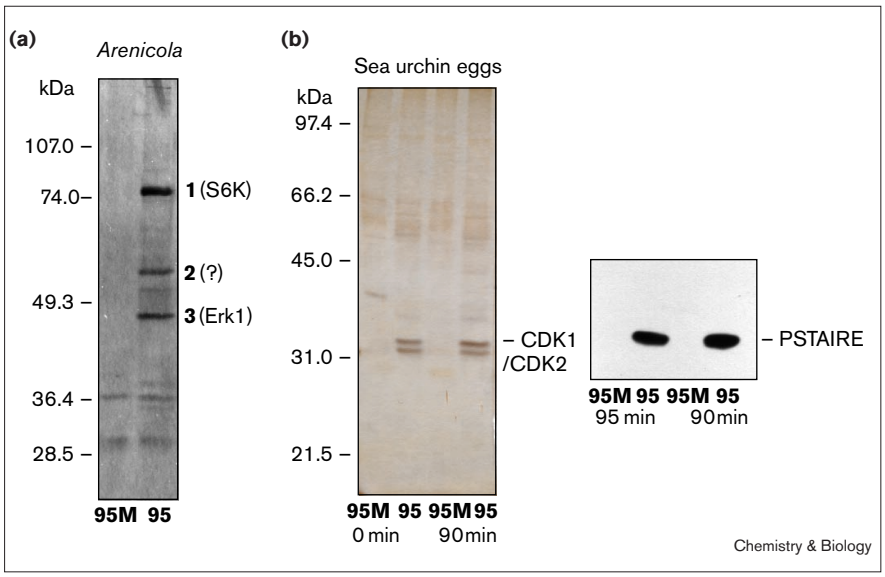

CDK1/cyclin B and three other proteins from lugworm oocytes and two proteins from sea urchin eggs bind to **95** matrix. Extracts from **(a)** lugworm metaphase oocytes or **(b)** sea urchin eggs were loaded on **95M** and **95** matrices. Bound proteins were resolved by SDS–PAGE and revealed by silver staining. Proteins **1**, **2** and **3** (lugworm) were further processed for microsequencing and identified as S6 kinase 2 (protein **1**) and Erk1 (protein **3**) (Figure 2). The sea urchin eggs provided two proteins, one of them co-migrating with CDK1/2 as revealed by immuno-reactivity with anti-PSTAIRE antibodies (right).

Figure 6

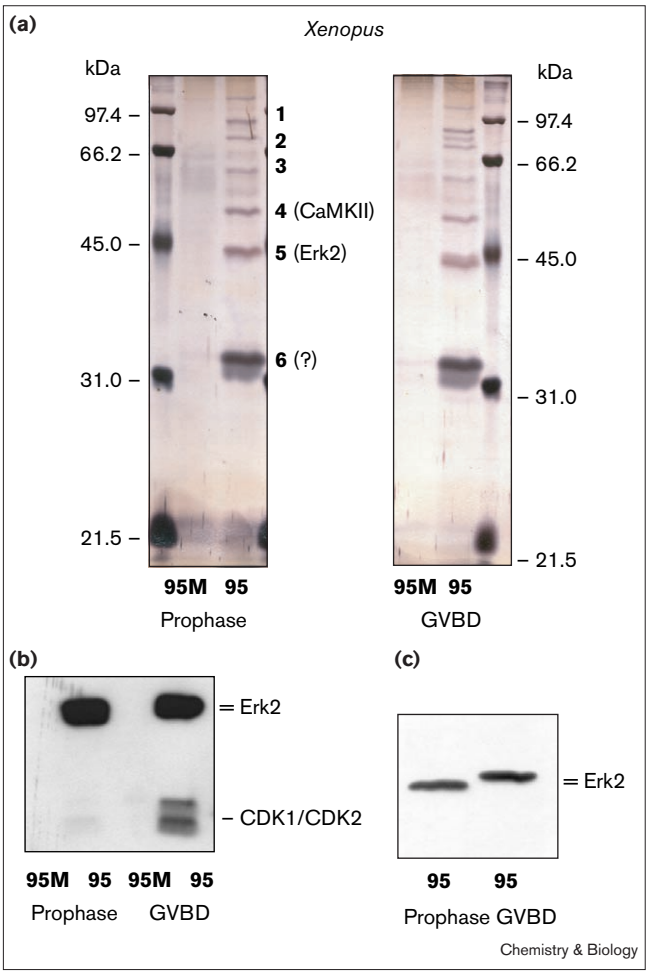

CDK1/cyclin B, Erk2 and six other proteins from *Xenopus* oocytes bind to **95** matrix. Extracts from *Xenopus* prophase (P) and maturing (GVBD, germinal vesicle breakdown) oocytes were loaded on **95M** and **95** matrices. Bound proteins were resolved by SDS–PAGE and revealed by **(a)** silver staining and **(b)** western blotting with anti-PSTAIRE and anti-erk2 antibodies. **(c)** The **95**-matrix-bound proteins were run on a modified electrophoresis system to allow visualisation of the mobility shift associated with Erk2 activation during maturation. Proteins **4** and **5** were further processed for microsequencing and identified as calmodulin-dependent kinase 2 and Erk 2, respectively (Figure 2).

Figure 7

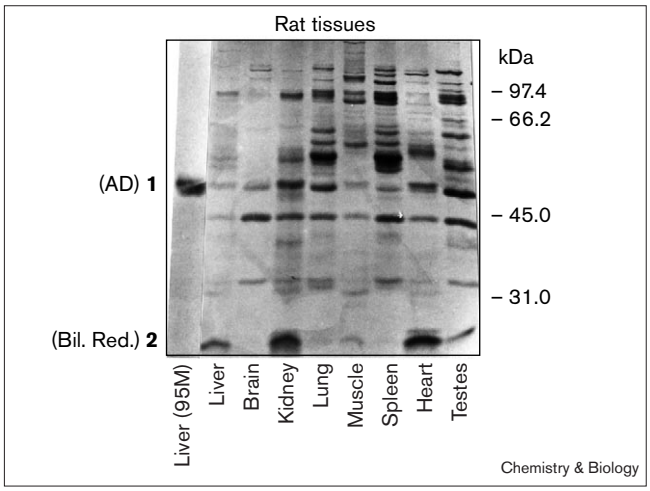

Proteins interacting with **95** matrix from various rat tissues. Extracts from liver, brain, kidney, lung, muscle, spleen, heart and testes were loaded on **95** matrix; a liver extract was also loaded on **95M** matrix. The bound proteins were resolved by SDS–PAGE, followed by silver staining. Protein **1** (liver extract on **95M** matrix) and protein **2** (liver extract on **95** matrix) were microsequenced and identified as alcohol dehydrogenase (AD) and biliverdin reductase (Bil. Red.), respectively (Figure 2).

human protozoan parasites (data not shown). In an effort to define the intraparasitic targets, the affinity chromatographic methods described above were applied to the following parasites: *Plasmodium falciparum*, *Leishmania mexicana*, *Trypanosoma cruzi* and *Toxoplasma gondii*. Extracts of each parasite species were loaded on **95M** and **95** matrices. The bound proteins were separated by SDS–PAGE and visualized by silver staining (Figure 10). A single 37 kDa protein in *Plasmodium* was found to bind specifically to the **95** matrix (Figure 10a). We formally identified it as *P. falciparum* casein kinase 1 (CK1) by microsequencing [44]. CK1 was also identified as a major **95**-binding protein in *L. mexicana* (Figure 10b) and in *T. cruzi* (Figure 10c). Two other proteins from *T. cruzi* had no known homologs (Figure 2). Finally, *T. gondii* provided a single principal **95**-binding protein (Figure 10d). It was also identified as CK1 by microsequencing (Figure 2). This protein was absent from **95** matrix loaded with an extract of the host Vero cells. In contrast, these cells provided a protein migrating at the level of Erk2 (confirmed by western blotting; data not shown).

Kinase selectivity of 95 and 97

The use of agarose-immobilised **95** as an affinity chromatography resin has allowed the identification of seven kinases that interact specifically with **95**, but not with **95M** (Figure 2). Although purvalanols were identified and optimised as selective CDK inhibitors, we re-examined the effect of **95** and its closely related, more cell-permeable analog, **97** (Figure 1), on the kinases identified as potential targets (Table 1). Roscovitine data are shown for comparison. Clearly, both **95** and **97** are very potent CDK inhibitors, with IC_{50} values of less than 10 and 40 nM, respectively. In contrast, they inhibit CK1, Erk1, Erk2, S6 kinase II and calmodulin-dependent kinase II only at much higher doses (IC_{50} between 3 and 15 μM). Other kinases are essentially insensitive including a variety of protein kinase C isoforms, cAMP and cGMP-dependent protein kinase, Raf kinase, c-jun amino-terminal kinase, insulin-receptor tyrosine kinase and v-abl [10,38]. Mammalian CK1 is only moderately inhibited by **95** and **97**. CK1 from the protozoan parasites may show a different sensitivity to these purines. Preliminary experiments with

Figure 8

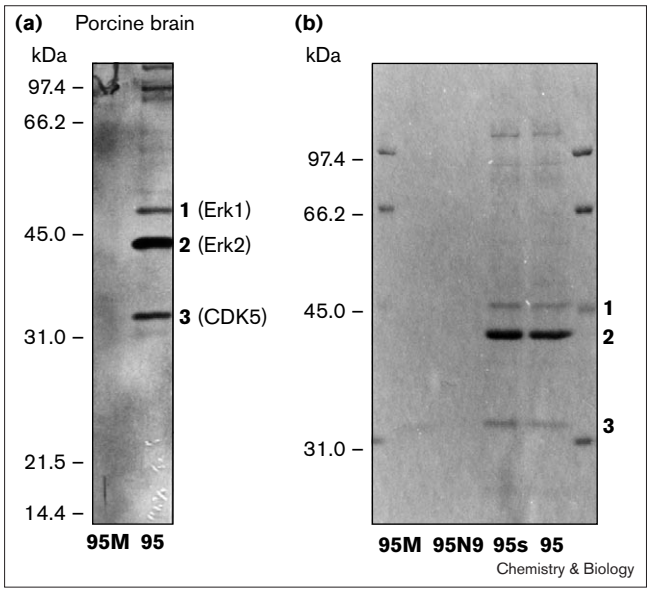

Three proteins from porcine brain interact with **95**. **(a)** Extracts from porcine brain were loaded on **95M** and **95** matrix. The bound proteins were resolved by SDS–PAGE, followed by silver staining. Proteins **1**, **2** and **3** were microsequenced and identified as Erk1, Erk2 and CDK5, respectively (Figure 2). **(b)** Extracts from porcine brain were loaded on **95M**, **95N9**, **95s** and **95** matrix. The bound proteins were resolved by SDS–PAGE, followed by Coomassie blue staining.

Figure 9

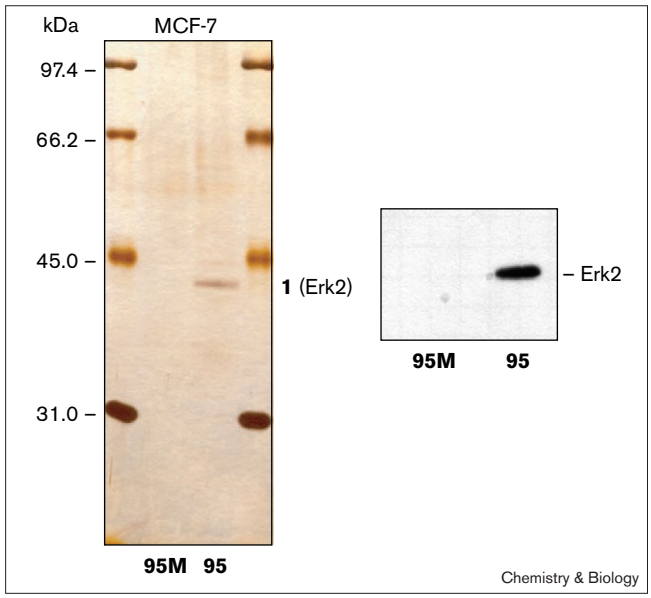

MCF-7 cells contain a principal **95**-binding protein. An MCF-7 cell line extract was loaded on **95M** and **95** matrices. The bound proteins were resolved by SDS–PAGE, followed by silver staining (left) or Western blotting with anti-Erk2 antibodies (right). Protein **1** was microsequenced and identified as Erk2 (Figure 2).

P. falciparum CK1 show a higher sensitivity to **95** (IC_{50} ~0.3 μM; data not shown).

Discussion

The use of immobilised **95** and **95M** has allowed the identification of three types of purine-binding proteins: proteins binding specifically to **95**, proteins binding selectively to **95M** and proteins binding to both resins.

The first category of proteins discovered by this study binds selectively to **95**, but not to **95M**. Besides biliverdin reductase (rat liver, but possibly also kidney and heart; see Figure 7), and some unidentified proteins, all **95**-selective proteins are kinases (seven were identified). According to a phylogenetic clustering of all kinases of known sequence [45], some of the kinases isolated specifically on the **95** matrix fall within a small subcluster of the so-called 'CMGC' group (CDK1, Erk 1 and Erk2), whereas others fall in the OPK group XII (CK1), CaM kinase group (CaMKII) and AGC subgroup VI (RS6K). The **95** matrix thus recognizes kinases of diverse structures. The ability to bind **95** matrix cannot be predicted by primary amino-acid sequence; however, the binding of both Erks and CDKs is in agreement with the crystal structure of CDK2 in complex with purines [46,47,15], and in particular with **95** [10] and with the crystal structure of olomoucine in complex with Erk2 [48] (the inhibitor shows an orientation which is almost the same as olomoucine and purvalanol in CDK2). In all crystal structures, the N6-benzylamino or N6-anilino substituents are situated towards the outside of the ATP-binding pocket, and are thus accessible to solvent (for review see [10]). Therefore, the orientation of **95** immobilised on the beads as shown in Figure 1 is still compatible with an interaction with kinases. A different orientation (**95** N9-linked matrix; Figure 1) would be incompatible with **95** binding to CDKs. As illustrated with porcine brain extracts (Figure 8), but also seen with starfish oocytes (data not shown), this orientation of **95**, with respect to agarose, totally abolishes the binding of proteins to **95** matrix. The crystal structures also tell us that the purine N6 acts as a hydrogen donor for the backbone carbonyl of Leu83. Methylation of N6 abolishes the possibility of such a hydrogen bond and introduces an unfavourable steric interaction that results in inactivation of the purine as a CDK inhibitor (see examples in [17,38]). The N6 methylation would therefore be expected to disrupt activity against any kinase that binds the inhibitor in an orientation similar to that observed in the CDK2–purvalanol B co-crystal structure. In fact, immobilised **95M** does not bind any of the **95**-binding kinases detected in this study showing that this methylation generically destroys kinase inhibitory activity as discussed above.

Alcohol dehydrogenase from rat liver is the only protein that we found to bind selectively to the **95M** matrix

Figure 10

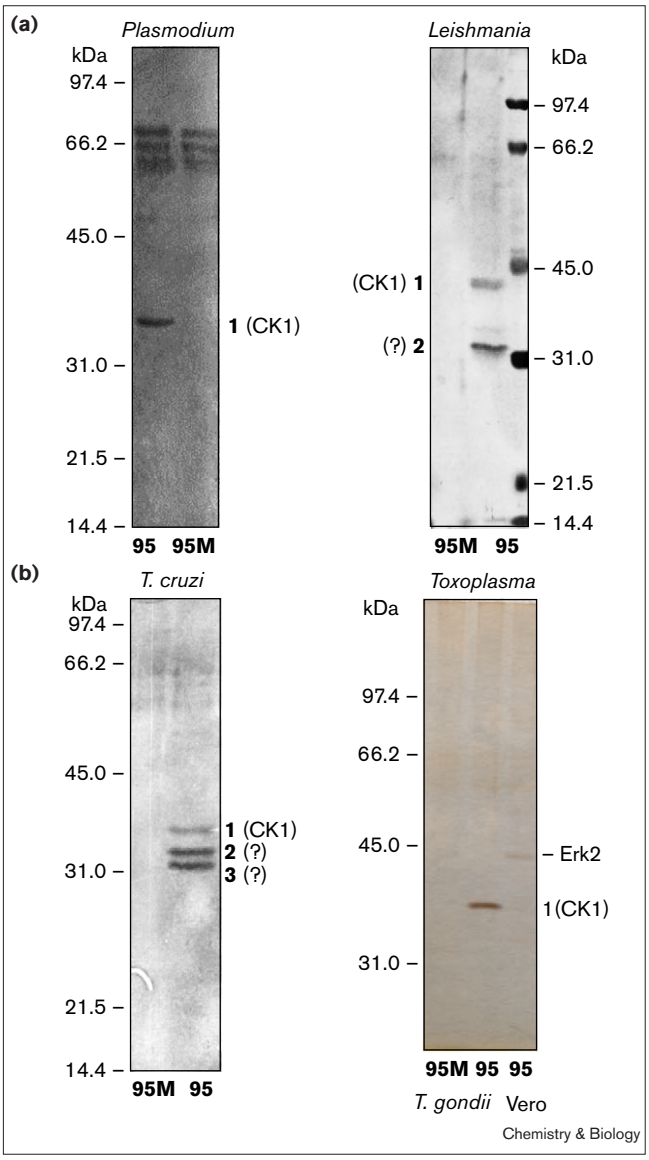

Human protozoan parasites. Extracts from **(a)** *P. falciparum*, **(b)** *L. mexicana*, **(c)** *T. cruzi* and **(d)** *T. gondii* were loaded on **95M** and **95** matrices. The bound proteins were resolved by SDS–PAGE, followed by silver staining. Proteins **1** from *P. falciparum, L. mexicana*, *T. cruzi* and *T. gondii* were identified as CK1 (Figure 2). For *Toxoplasma*, extracts of uninfected Vero cells were also loaded on the affinity matrices (right).

(Figure 7). A trace of a protein with similar electrophoretic mobility was observed on **95** matrix loaded with rat liver extract. All other tissues and cells that we tested did not contain any **95M**-specific binding proteins. The presence of alcohol dehydrogenase in liver, and its binding to an alcohol containing molecule such as purvalanol, is not a surprise.

We encountered very few proteins interacting with both resins. In the starfish oocyte example, a major 32 kDa protein binds to **95** and **95M** matrices, but also to $p9^{CKShs1}$ beads (Figure 3). Its intensity is reduced after a passage on any type of beads, including control ethanolamine-sepharose, prior to loading on **95** matrix (Figure 4). This ligand-independent binding suggests direct interactions with agarose.

Table 1

Selectivity of 95, 97 and roscovitine.

Enzyme	**95**	**97**	Roscovitine
CDK1/cyclin B	0.006	0.033	0.450
CDK2/cyclin A	0.006	0.028	0.700
CDK5/p25	0.006	0.020	0.160
CK1 (mammalian)	>3.333	3.000	n.d.
Erk1	3.333	12.000	34.000
Erk2	1.000	2.400	14.000
S6 kinase (p70rsk)	15.000	8.300	130.000
CaM kinase II	13.000	5.500	32.000

The purified enzymes were assayed in the presence of an increasing concentration of the inhibitors. The IC_{50} values was evaluated graphically and are presented in μM; n.d., not determined. CDK1/cyclin B is a native kinase from starfish oocytes, all other kinases are recombinant mammalian enzymes.

The presence of very few proteins on immobilised **95**, as shown in the variety of models presented here, is consistent with the strong selectivity exhibited by purvalanols, in particular, and by 2,6,9-trisubstituted purines, in general. The molecular basis for this exquisite selectivity still remains to be understood. One important determinant is the ability of the subset of kinases that can bind to purvalanol to accommodate a bulky N6 group. Although this can be validated only for the kinases whose crystal structures have been solved (CDK2, Erk2 and CK1) it is also likely to be true for CaMKII and the RS6K. The identification on **95** matrix of kinases other than CDKs raises several questions. Why do these kinases, which are less sensitive to purines (Table 1), bind to the **95** matrix? Is their lower affinity compensated by their cellular abundance? Why, then, are there not more proteins binding to the affinity matrix? Are some of these cellular kinases modified post-translationally in such a way that their affinity is enhanced compared with the *in vitro* expressed kinases? The IC_{50} values have been determined on recombinant enzymes that may be partially inactive owing to improper folding or lack of adequate post-translational modifications. A substantial proportion of the kinase may still have the ability to trap the inhibitor while lacking kinase activity. This would result in an apparent increase of the IC_{50} value. Would specific inhibition of these apparently low-affinity kinases enhance the *in vivo* efficiency of purvalanols on CDKs? Erk1/2, RS6K and CaMKII are likely to be expressed in most if not all the tissues that we examined in this study. Why are they not recovered on **95**

matrix from all samples? There could be several reasons for this, for example slight sequence differences that could modify the affinity, different post-translational modifications or binding of various regulating proteins, which could affect the interaction with the inhibitor, significant variations in their abundance; or a combination of these factors. In any case, interpretation of any cellular effects of purvalanols clearly has to take into account the pattern of **95** binding proteins, as detected by our method. We feel that this method validates the intracellular targets of **95** and provides a general approach to identify intracellular targets of a defined compound. As an example, we have shown that, despite their structural similarity, a few purines (**52, 97, 212**) have different cellular effects (arrest in M, in G2 and induction of apoptosis, respectively) [38]. Immobilisation of these compounds and affinity-chromatography purification of interacting proteins from a cellular extract should provide a pattern of proteins specific to each compound. These patterns of bound proteins might allow the identification of the specific target(s) responsible for each specific cellular effect.

The results obtained with protozoan parasites have to be discussed separately. Indeed, we anticipated that their CDKs would be divergent enough from mammalian CDKs to present significant differences in sensitivity to purvalanols. So far we have not identified any CDK-related kinases on the **95** matrix, despite their definitive presence in protozoan parasites [49]. Surprisingly, CK1 was detected on **95** matrix loaded with extracts of four different species of parasites. This raises several questions. Why did we never detect any **95**-binding CK1 with mammalian tissues? What is the molecular basis for this difference, despite the extreme conservation of CK1 structure? Are the affinities of protozoan CK1 for purvalanols, and thereby their sensitivity to these compounds, much higher? If this were the case, CK1s from protozoan parasites would be promising screening targets for the identification of new molecules effective against protozoan parasites. The cloning, expression and testing of these CK1s, and their comparison with their mammalian homologs, is an obvious priority for us. The *P. falciparum* CK1 gene has already been characterised [44]; we are currently performing experiments to determine its *in vitro* susceptibility to **95** and related purines.

The presence of a very limited set of **95**-binding proteins in brain is encouraging. Interested by the design of compounds active against neurodegenerative disorders, we are mostly looking for inhibitors of CDK5 and GSK-3. Given the interaction of Erk1/Erk2 with purvalanols shown here, the screening for CDK5 inhibitors should incorporate a parallel screen with Erk1/Erk2. Whole brain extracts were used in this study. We clearly need to study the pattern of **95**-binding proteins in various regions of the brain, after precise anatomical dissections. Also, the comparison of **95**-binding proteins obtained from nervous tissues representative of various pathological situations may reveal new targets to go after.

The oocytes and eggs presented in this study constitute powerful models for the study of cell-cycle regulation. Identification of their purvalanol targets will allow a better comprehension of some cellular processes involved in control of cell division. It will also facilitate the optimisation of new anti-mitotic compounds of therapeutic potential in cancer.

Finally, identification of **95**-binding proteins in liver provides some clues on the metabolism of purvalanols by a whole organism. This may help in the design of more metabolism-resistant compounds, and in the understanding and possibly avoidance of undesired side effects of purvalanols.

In summary, we have designed a simple batch affinity chromatography method that allows the rapid purification, detection and identification of intracellular targets of CDK inhibitors. This method has been successfully applied to purvalanols, but could be extended to all other known CDK inhibitors, in particular those that have been co-crystallised with CDK2. This purification method could readily be adapted to a 96-well format whereby a library of immobilized purine compounds could be screened to identify multiple targets in parallel. This approach would allow the unbiased identification of potential targets for the library as a whole, as well as specific library members. Indeed this approach might be applied to combinatorial libraries of other directed scaffolds (e.g. statine derivatives, hydroxamates) to rapidly identify inhibitor–receptor pairs on a genome-wide level. Furthermore, knowledge of the pattern of target proteins allows a better interpretation of the cellular effects of the inhibitors and will also help in orientating the optimisation of compounds for therapeutic applications against cancer, neurodegenerative disorders and protozoan parasites.

Significance

Chemical inhibitors of cyclin-dependent kinases (CDKs) have great therapeutic potential against various proliferative and neurodegenerative disorders. The founding member of the family of 2,6,9-trisubstituted purines, olomoucine, has been optimized for activity against CDK1/cyclin B by combinatorial and medicinal chemistry efforts to yield the purvalanol inhibitors (IC_{50} = 6 nM). Despite their excellent *in vitro* selectivity against a collection of 25 purified kinases and numerous cell-based studies that support their action against CDKs, their actual intracellular targets remain unverified. To address this question, purvalanol B (95) and a N6-methylated, CDK-inactive derivative (95M) were immobilized to an agarose matrix. Extracts from a

diverse collection of cell types and organisms were screened for purvalanol-B-binding proteins. In addition to validating CDKs as intracellular targets, a variety of protein kinases (Erk1, Erk2, RS6K, CaMKII and CK1) were specifically recovered from the **95** matrix. Several of the recovered kinases, including CaMKII, Erk1 and Erk2, were inhibited by the purvalanols with IC_{50} values 1000-fold higher than those measured for CDK1, 2 and 5, suggesting that their isolation may result from higher cellular abundance. CK1 was identified as one of the principal **95**-matrix binding proteins in *Plasmodium falciparum*, *Trypanosoma cruzi*, *Leishmania mexicana* and *Toxoplasma gondii*. Purvalanol compounds were also shown to inhibit the proliferation of these parasites, suggesting that CK1 may serve as a valuable target for further screening with libraries of 2,6,9-trisubstituted purines. The ease with which a simple batchwise affinity chromatography approach using two purine derivatives resulted in the isolation of a small set of highly purified and related kinases suggests that this approach may serve as a general method for identifying the intracellular targets of a given ligand.

Materials and methods

Preparation of extracts

Various biological materials were used in this study (see Supplementary material): starfish and *Arenicola* oocytes, sea urchin eggs, *Xenopus* oocytes and gonads, rat tissues, porcine brain, MCF-7 cells, protozoan parasites (*Plasmodium falciparum*, *Trypanosoma cruzi*, *Leishmania mexicana*, *Toxoplasma gondii*). Tissues were weighed, homogenised and sonicated in homogenisation buffer (2 ml per gram of material). Homogenates were centrifuged for 10 min at 14,000*g* and 4°C. The supernatant was recovered and immediately loaded on the affinity matrices. Cells were directly sonicated in homogenisation buffer and processed the same way.

Preparation and use of affinity reagents

Purines (**95**, **95M**) were coupled to Reactigel® agarose beads at a calculated final concentration of 10–50 μmol/ml of resin. They were stored at 4°C as a 33% (v/v) slurry in bead buffer. Just before use, 10 μl of packed beads were washed with 1 ml of bead buffer and resuspended in 400 μl of this buffer. The cell/tissue supernatant (400 μl) was then added; the tubes were rotated at 4°C for 30 min. After a brief spin at 10,000*g* and removal of the supernatant, the beads were washed four times with bead buffer before addition of 50 μl of 2× Laemmli sample buffer. When larger samples were prepared for microsequencing, up to 25 ml of cell/tissue extracts were incubated with 200–500 μl packed beads and 25 ml of bead buffer. The beads were processed as described above and the bound proteins were recovered with 300 μl of 2× Laemmli sample buffer.

The CDK1/2-binding protein $p9^{CKShs1}$ was purified from an overproducing strain of *Escherichia coli* and conjugated to CNBr-activated sepharose 4B as described [40] at a concentration 3.9 mg $p9^{CKShs1}$ per microlitre of gel (i.e. 0.5 μmol/ml of gel). $P9^{CKShs1}$-sepharose beads were kept at 4°C as a 20% (v/v) suspension in bead buffer. Cell extracts (400 μl) were incubated with 10 μl packed beads + 400 μl bead buffer for 30 min. The beads were processed as described for the purine beads.

Supplementary material

Supplementary material including details on chemicals and antibodies, buffers, biological material, electrophoresis and western blotting, identification of purified proteins and kinase assays is available at http://current-biology.com/supmat/supmatin.htm.

Acknowledgements

We are grateful to D. Alessi, M. Cobb, W. Harper, J. Bibb, W. Harper, P. Loyer, L.A. Patterson, L. Pinna, J.H. Wang and M. Yamashita for providing reagents. We thank the fishermen of the 'Station Biologique de Roscoff' for collecting the starfish and sea urchins, and H. Ronné for the photographic work. This work would not have been possible without the appreciated expert protein microsequencing work of J. d'Alayer and M. Davi, from the Pasteur Institute. This research was supported by grants from the Association pour la Recherche sur le Cancer (ARC 9314) (to L.M.) and the Conseil Régional de Bretagne (to L.M.). M.K. was supported by a DEA fellowship from the Université de Bretagne Occidentale. The work on *P. falciparum* benefitted from the support of the INCO-DC programme (contract IC18-CT97-0217) (C.D. and L.M.) of the French Ministère de l'Education Nationale, de la Recherche et de la Technologie (C.D. and L.M.) and from the UNDP/World Bank/WHO Special Program for Research and Training in Tropical Diseases (TDR). M.S. and J.F.D. were supported by a Sidaction grant.

References

1. Dunphy, W.G. (ed.) (1997). Cell cycle control. *Methods Enzymol.*, **283**, 678.
2. Morgan, D. (1997). Cyclin-dependent kinases: engines, clocks, and microprocessors. *Annu. Rev. Cell Dev. Biol.* **13**, 261-291.
3. Vogt, P.K. & Reed, S.I. (1998). Cyclin dependent kinase (CDK) inhibitors. *Curr. Top. Microbiol. Immunol.* **227**, 1-169.
4. Stein, G.S., Baserga, R., Giordano, A. & Denhardt, D.T. (1999). The *Molecular Basis of Cell Cycle and Growth Control.* Wiley-Liss Inc., New York.
5. Senderowicz, A., *et al.*, & Sausville, E.A. (1998). Phase I trial of continuous infusion flavopiridol, a novel cyclin-dependent kinase inhibitor, in patients with refractory neoplasms. *J. Clin. Oncol.* **16**, 1-17.
6. Garrett, M.D. & Fattaey, A. (1999). CDK inhibition and cancer therapy. *Curr. Opin. Genet. Dev.* **9**, 104-111.
7. Meijer, L. (1996). Chemical inhibitors of cyclin-dependent kinases. *Trends Cell Biol.* **6**, 393-397.
8. Meijer, L. & Kim, S.H. (1997). Chemical inhibitors of cyclin-dependent kinases. *Methods Enzymol.*, **283**, 113-128.
9. Meijer, L., Leclerc, S. & Leost, M. (1999). Properties and potential applications of chemical inhibitors of cyclin-dependent kinases. *Pharmacol. Ther.* **82**, 279-284.
10. Gray, N.S., Détivaud, L., Doerig, C. & Meijer, L. (1999). ATP-site directed inhibitors of cyclin-dependent kinases. *Curr. Med. Chem.* **6**, 859-875.
11. Rialet, V. & Meijer, L. (1991). A new screening test for antimitotic compounds using the universal M phase-specific protein kinase, $p34^{cdc2}$/cyclin B^{cdc13}, affinity-immobilized on $p13^{suc1}$-coated microtitration plates. *Anticancer Res.* **11**, 1581-1590.
12. Kitagawa, M., *et al.*, & Okuyama, A. (1993). Butyrolactone I, a selective inhibitor of cdk2 and cdc2 kinase. *Oncogene* **8**, 2425-2432.
13. Vesely, J., *et al.*, & Meijer, L. (1994). Inhibition of cyclin-dependent kinases by purine derivatives. *Eur. J. Biochem.* **224**, 771-786.
14. Losiewiecz, M.D., Carlson, B.A., Kaur, G., Sausville, E.A. & Worland, P.J. (1994). Potent inhibition of cdc2 kinase activity by the flavonoid L86-8275. *Biochem. Biophys. Res. Commun.* **201**, 589-595.
15. De Azevedo, W.F., Leclerc, S., Meijer, L., Havlicek, L., Strnad, M. & Kim, S-H. (1997). Inhibition of cyclin-dependent kinases by purine analogues: crystal structure of human cdk2 complexed with roscovitine. *Eur. J. Biochem.* **243**, 518-526.
16. Meijer, L., *et al.*, & Moulinoux, J.P. (1997). Biochemical and cellular effects of roscovitine, a potent and selective inhibitor of the cyclin-dependent kinases cdc2, cdk2 & cdk5. *Eur. J. Biochem.* **243**, 527-536.
17. Gray, N.S., *et al.*, & Schultz P.G. (1998). Exploiting chemical libraries, structure, and genomics in the search for kinase inhibitors. *Science* **281**, 533-538.
18. Hoessel, R., *et al.*, & Meijer, L. (1999). Indirubin, the active constituent of a Chinese antileukaemia medicine, inhibits cyclin-dependent kinases. *Nat. Cell Biol.* **1**, 60-67.
19. Schultz, C., *et al.*, & Kunick C. (1999). The Paullones, a series of cyclin-dependent kinase inhibitors: synthesis, evaluation of CDK1/cyclin B inhibition, and *in vitro* antitumor activity. *J. Med. Chem.* **42**, 2909-2919.
20. Zaharevitz, D., *et al.*, & Sausville, E.A. (1999). Discovery and initial characterization of the paullones, a novel class of small-molecule inhibitors of cyclin-dependent kinases. *Cancer Res.* **59**, 2566-2569.

21. Meijer, L., *et al*., & Pettit, G.R. (2000). Inhibition of cyclin-dependent kinases 1, 2 & 5, GSK-3β and casein kinase 1 by hymenialdisine, a marine sponge constituent. *Chem. Biol.* **7**, 51-63
22. Brooks, E.E., *et al*., & Shiffman, D. (1997). CVT-313, a specific and potent inhibitor of CDK2 that prevents neointimal proliferation. *J. Biol. Chem.* **272**, 29207-29211.
23. Suzuki, J.I., *et al*., & Sekiguchi, M. (1997). Prevention of graft coronary arteriosclerosis by antisense cdk2 kinase oligonucleotide. *Nature Med.* **3**, 900-903
24. Pippin, J.W., Qu, Q., Meijer, L. & Shankland, S.J. (1997) Direct *in vivo* inhibition of the nuclear cell cycle cascade in experimental mesangial proliferative glomerulonephritis with roscovitine, a novel CDK2 antagonist. *J. Clin. Invest.* **100**, 2512-2520.
25. Shankland, S.J. (1997). Cell-cycle control and renal disease. *Kidney Int.* **52**, 294-308.
26. Bresnahan, W.A., Boldogh, I., Chi, P., Thompson, E.A. & Albrecht, T. (1997). Inhibition of cellular cdk2 activity blocks human cytomegalovirus replication. *Virology* **231**, 239-247.
27. Mancebo, H.S.Y., *et al*., & Flores, O. (1997). P-TEFb kinase is required for HIV Tat transcriptional activation *in vivo* and *in vitro*. *Genes Dev.* **11**, 2633-2644.
28. Schang, L.M., Phillips, J. & Schaffer, P.A. (1998). Requirement for cellular cyclin-dependent kinases in herpes simplex virus replication and transcription. *J. Virol.* **72**, 5626-5637.
29. Ye, M., Duus, K.M., Peng, J., Price, D.H. and Grose, C. (1999). Varicella-zoster virus Fc receptor component gI is phosphorylated on its endodomain by a cyclin-dependent kinase. *J. Virol.* **73**, 1320-1330
30. Imahori, K. & Uchida, T. (1997). Physiology and pathology of tau protein kinases in relation to Alzheimer's disease. *J. Biochem.* **121**, 179-188.
31. Mandelkow, E.-M. & Mandelkow, E. (1998). Tau in Alzheimer's disease. *Trends Cell Biol.* **8**, 425-427.
32. Meijer, L. & Pondaven, P. (1988). Cyclic activation of histone H_1 kinase during the sea urchin egg mitotic divisions. *Exp. Cell Res.* **174**, 116-129.
33. Néant, I., & Guerrier, P. (1988). 6-Dimethylaminopurine blocks starfish oocyte maturation by inhibiting a relevant protein kinase activity. *Exp. Cell Res.* **176**, 68-79.
34. Legraverend, M., Ludwig, O., Bisagni, E., Leclerc, S. & Meijer, L. (1998). Synthesis of C2 alkynylated purines, a new family of potent inhibitors of cyclin-dependent kinases. *Bioorg. Med. Chem. Lett.* **8**, 793-798.
35. Norman, T.C., Gray, N.S., Koh, J.T. & Schultz, P.G. (1996). A structure-based library approach to kinase inhibitors. *J. Am. Chem. Soc.* **118**, 7430-7431
36. Gray, N.S. & Schultz, P.G. (1997). Combinatorial synthesis of 2,9-substituted purines. *Tetrahedron Lett.* **38**, 1161-1164.
37. Nugiel, D.A., Cornelius, L.A.M. & Corbett, J.W. (1997). Facile preparation of 2,6-disubstituted purines using solid phase chemistry. *J. Org. Chem.* **62**, 201-203.
38. Chang, Y.T., *et al*., & Schultz, P.G. (1999). Synthesis and application of 2,6,9-trisubstituted purine library towards the development of functionally diverse CDK inhibitors. *Chem. Biol.* **6**, 361-375.
39.. Meijer, L. and Mordret, G. (1994). Starfish oocyte maturation: from prophase to metaphase. *Semin. Dev. Biol.* **5**, 165-171.
40. Borgne, A. & Meijer, L. (1996). Sequential dephosphorylation of $p34^{cdc2}$ on its Thr-14 and Tyr-15 residues at the prophase/metaphase transition. *J. Biol. Chem.* **271**, 27847-27854.
41. Meijer, L. & Durchon, M. (1977). Contrôle neurohormonal de la maturation des ovocytes chez *Arenicola marina* (Annélide Polychète). Etude *in vitro* [Neurohormonal control of oocyte maturation in *Arericola marina*: *in vivo* study]. *C.R. Acad. Sci. Paris* **285**, 377-380.
42. Meijer, L., Azzi, L. & Wang, J.Y.J. (1991). Cyclin B targets $p34^{cdc2}$ for tyrosine phosphorylation. *EMBO J.* **10**, 1545-1554.
43. Rosania, G.R., Merlie, J., Gray, N., Chang, Y-T., Schultz, P.G. & Heald, R. (1999). A cyclin-dependent kinase inhibitor inducing cancer cell differentiation: biochemical identification using Xenopus egg extracts. *Proc. Natl. Acad. Sci. USA* **96**, 4797-4802.
44. Barik, S., Taylor, R.E. & Chakrabarti, D. (1997). Identification, cloning, and mutational analysis of the casein kinase 1 cDNA of the malaria parasite, *Plasmodium falciparum*. *J. Biol. Chem.* **272**, 26132-26138
45. Hanks, S.K. & Hunter T. (1995). The eukaryotic protein kinase superfamily: kinase (catalytic) domain structure and classification. *FASEB J.* **9**, 576-596.
46. Schulze-Gahmen, U., *et al*., and Kim, S.-H. (1995). Multiple modes of ligand recognition: crystal structures of cyclin-dependent protein kinase 2 in complex with ATP and two inhibitors, olomoucine and isopentenyladenine. *Proteins* **22**, 378-391.
47. Schulze-Gahmen, U., De Bondt, H.L. & Kim, S.-H. (1996). High-resolution crystal structures of human cyclin-dependent kinase 2 with and without ATP: bound waters and natural ligand as guides for inhibitor design. *J. Med. Chem.* **39**, 4540-4546
48. Wang, Z., *et al*., & Goldsmith, E.J. (1998). Structural basis of inhibitor selectivity in MAP kinases. *Structure* **6**, 1117-1128.
49. Doerig, C., Chakrabarti, D., Kappes, B. & Matthews, K. (2000). The cell cycle in protozoan parasites. In *Progress in Cell Cycle Research* (Meijer, L., Jezequel, A. & Ducommun, B., eds.), vol. 4, pp163-183, Plenum Press, New York.

Supplementary material

Intracellular targets of cyclin-dependent kinase inhibitors: identification by affinity chromatography using immobilised inhibitors

M Knockaert, N Gray, E Damiens, Y-T Chang, P Grellier, K Grant, D Fergusson, J Mottram, M Soete, J-F Dubremetz, K Le Roch, C Doerig, PG Schultz and L Meijer

Chemistry & Biology 2000, **7**:411–422

Supplementary materials and methods

Chemicals and antibodies

Sodium ortho-vanadate, 1-methyladenine, EGTA, EDTA, MOPS, β-glycerophosphate, dithiothreitol (DTT), sodium fluoride, p-nitrophenyl phosphate, leupeptin, aprotinin, soybean trypsin inhibitor, benzamidine, formaldehyde, β-mercaptoethanol, HEPES, Na_2CO_3, phenylphosphate, amidoblack, Tween-20, CNBr-activated sepharose 4B, collagenase were obtained from Sigma Chemicals. Nonidet P-40 was from Fluka, dispase from Boehringer, and MS222 from Pag Industries. Acrylamide/bis-acrylamide (30/0.8) was from Genomic Solutions. Electrophoresis reagents, the 'Silver Stain Plus' kit, protein assay reagent and horseradish peroxidase-coupled anti-mouse antibodies were purchased from BioRad. Reactigel® 6X (1,1′-carbonyldiimidazole-activated 6% crosslinked beaded agarose) was obtained from Pierce. Monoclonal antibodies against H_2N-EGV*PSTAIRE*SLLKEGGC-COOH ('anti-PSTAIRE' antibodies) and against *Bufo* cyclin B were kindly provided by M. Yamashita. **95**, **95M**, **97** and **97M** were prepared as previously described [S1]. **95** and **95M** with a sidechain were prepared as previously described [S2]. They were bound to a final concentration of 19.1 μmole/ml settled resin.

Buffers

Homogenisation buffer. Homogenisation buffer contained 60 mM β-glycerophosphate, 15 mM p-nitrophenyl phosphate, 25 mM MOPS (pH 7.2), 15 mM EGTA, 15 mM MgCl2, 1 mM DTT, 1 mM sodium orthovanadate, 1 mM sodium fluoride, 1 mM phenyl phosphate, 10 μg/ml leupeptin, 10 μg/ml aprotinin, 10 μg/ml soybean trypsin inhibitor and 100 μM benzamidine.

Buffer C. Buffer C was as the homogenisation buffer but with 5 mM EGTA and no NaF nor protease inhibitors.

Bead buffer. Bead buffer contained 50 mM Tris (pH 7.4), 5 mM NaF, 250 mM NaCl, 5 mM EDTA, 5 mM EGTA, 0.1% Nonidet P-40, 10 μg/ml leupeptin, 10 μg/ml aprotinin, 10 μg/ml soybean trypsin inhibitor and 100 μM benzamidine.

Tris-buffered saline/Tween-20. Tris-buffered saline contained 50 mM Tris pH 7.4, 150 mM NaCl and 0.1% Tween-20.

Sodium bicarbonate buffered saline. Sodium bicarbonate buffered saline contained 200 mM $NaHCO_3$ pH 8.2 and 200 mM NaCl.

Merriam's medium. Merriam's medium contained 10 mM HEPES pH 7.6, 88 mM NaCl, 1 mM KCl, 0.33 mM $Ca(CO_3)_2$, 0.41 mM $CaCl_2$ and 0.82 mM $MgSO_4$.

Leishmania mexicana *culture buffer.* L.m. buffer contained 1× M199 (Gibco), 20 mM sodium bicarbonate, 200 mM HEPES (pH 7.4), 0.5 mM adenine and 0.0025% Hemin.

Biological material

Starfish oocytes. The starfish *Marthasterias glacialis* were collected by dredging in Brittany and kept under running seawater until use. For large-scale preparations of oocyte extracts, gonads were removed from mature starfish, and either directly frozen in liquid N_2 and kept at –80°C (P, prophase oocytes) or incubated with 10 μM 1-methyladenine in Millipore-filtered natural sea water for 30 min (M, metaphase oocytes). By that time all the oocytes had entered the M phase and were expelled from the gonads. They were recovered by gentle centrifugation, rapidly frozen in liquid N_2 and kept at –80°C (for experimental details see [S3]).

Arenicola oocytes. The lugworm *Arenicola defodiens* was induced to spawn and metaphase-arrested oocytes were collected by centrifugation, rapidly frozen in liquid N_2 and kept at –80°C (courtesy of L.A. Patterson).

Sea urchin eggs. The sea urchins *Sphaerechinus granularis* were obtained by diving in northern Brittany. Egg spawning were induced by injection of 0.5 ml of 0.2 M acetylcholine through the perribuccal membrane. Eggs were washed with Millipore-filtered natural sea water and fertilised as previously described [S4]. Unfertilised or metaphase (90 min post-fertilisation) eggs were pelleted and frozen in liquid nitrogen.

Xenopus oocytes and gonads. Female *Xenopus laevis* were anaesthetised in MS 222 (1 g/l). Their gonads were removed and incubated with dispase (0.4 mg/ml) in Merriam's medium for 4 h, then with collagenase (0.8 mg/ml) in Merriam's medium for 30–45 min to remove the follicle cells. The prophase-arrested oocytes were rinsed in Merriam's medium and kept in this buffer until further use. Oocyte maturation was triggered by incubation with 1 μM progesterone; matured oocytes were collected after germinal vesicle breakdown (6 h). Under some circumstances, whole gonads were used for affinity purifications.

Rat tissues. The liver, brain, heart, muscles, spleen, testes, lungs and kidneys of mature rats (*Rattus norvegicus*) were provided by P. Loyer. They were stored at –80°C until protein extraction and affinity chromatography.

Porcine brain. Porcine brains were obtained from a local slaughterhouse and either directly homogenised and processed for affinity chromatography or stored at –80°C until use.

MCF-7 cells. MCF-7 cells were cultured as described elsewhere [S5].

Protozoan parasites. Four different protozoan parasites were cultivated under specific conditions and pelleted before freezing at –80°C. The cell pellets were extracted with homogenisation buffer just prior to affinity chromatography.

Plasmodium falciparum. The clone 3D7 [S6] was grown in human erythrocytes using the method of Zolg *et al.* [S7], except that the culture medium contained 0.5% Albumax (Life Technologies) instead of human serum. Parasite pellets were obtained by lysis of the erythrocyte membranes in 0.15% saponin in PBS followed by centrifugation and several washes with PBS, and were then resuspended in homogenisation buffer.

Trypanosoma cruzi. Epimastigote forms of the Y strain were maintained and grown in liver infusion medium, containing 10% fetal calf serum, at 28°C and under continuous agitation [S8]. After three washes in PBS, cells were lysed in homogenisation buffer by three cycles of freezing and thawing. Homogenates were centrifuged for 30 min at 10,000*g* and 4°C and stored frozen at –80°C.

Leishmania mexicana. Cells were grown from a first sub-passage liquid-nitrogen stock of lesion amastigotes (MNYC/BZ/62/M379). They were cultivated in 500 ml *L. mexicana* medium bottles, at 25°C, to a density of 5×10^6 to 1×10^7 ml, pelleted and frozen.

Toxoplasma gondii. Host Vero cells were cultivated in DMEM medium containing 3% fetal calf serum, with 5% CO_2 at 37°C. Cells were infected (30×10^6 per 150 cm^2 flask) in this medium. After 48 or 72 h, parasites (about 10^9 per flask) were purified on glass fibres after lysis of the host cells. They were washed with PBS, pelleted, frozen and kept at –80°C.

Preparation of extracts
Tissues were weighed, homogenised and sonicated in homogenisation buffer (2 ml per gram of material). Homogenates were centrifuged for 10 min at 14,000*g* and 4°C. The supernatant was recovered and immediately loaded on the affinity matrices. Cells were directly sonicated in homogenisation buffer and processed the same way.

Preparation and use of affinity reagents
Purines (**95**, **95M**) were coupled to Reactigel® agarose beads at a calculated final concentration of 10–50 μmol/ml of resin. They were stored at 4°C as a 33% (v/v) slurry in bead buffer. Just before use, 10 μl of packed beads were washed with 1 ml of bead buffer and resuspended in 400 μl of this buffer. The cell/tissue supernatant (400 μl) was then added; the tubes were rotated at 4°C for 30 min. After a brief spin at 10,000*g* and removal of the supernatant, the beads were washed four times with bead buffer before addition of 50 μl of 2× Laemmli sample buffer. When larger samples were prepared for microsequencing, up to 25 ml of cell/tissue extracts were incubated with 200–500 μl packed beads and 25 ml of bead buffer. The beads were processed as described above and the bound proteins were recovered with 300 μl of 2× Laemmli sample buffer.

The CDK1/2-binding protein $p9^{CKShs1}$ was purified from an overproducing strain of *Escherichia coli* and conjugated to CNBr-activated sepharose 4B as described [S3] at a concentration 3.9 mg $p9^{CKShs1}$ per microlitre of gel (i.e. 0.5 μmol/ml) of gel. $P9^{CKShs1}$-sepharose beads were kept at 4°C as a 20% (v/v) suspension in bead buffer. Cell extracts (400 μl) were incubated with 10 μl packed beads + 400 μl bead buffer for 30 min. The beads were processed as described for the purine beads.

Electrophoresis and western blotting
Proteins bound to **95**, **95M** matrix or $p9^{CKShs1}$-sepharose beads were recovered with 2× Laemmli sample buffer. After heat denaturation for 3 min, the bound proteins were separated by 10% SDS–PAGE (0.7 mm thick gels), followed by immunoblotting analysis, silver or Coomassie blue staining. To visualise the shift of Erk2 electrophoretic mobility associated with its activation, the acrylamide/bis-acrylamide ratio was 29.8/0.18 instead of the usual 30/0.8. Silver staining was performed using either the Biorad 'Silver Stain Plus' kit or a home recipe (fixative: 250 μl 37% formaldehyde in 250 ml 50% methanol; rinsing with milliQ water containing 35 μM DTT, followed by 0.1% $AgNO_3$ in milliQ water (w/v); developer: 12 g Na_2CO_3 in 400 ml milliQ water containing 200 μl 37% formaldehyde). When samples were prepared for microsequencing, gels (1.5 mm thick) were stained with amidoblack (3 mg per 100 ml of methanol/acetic acid/water, 25/5/20). For immunoblotting, proteins were transferred to 0.1 μm nitrocellulose filters (Schleicher and Schull). These were blocked with 5% low-fat milk in Tris-buffered saline/Tween-20, incubated with anti-PSTAIRE (1:2000; 1 h) or anti-cyclin B (1:1000; 1 h) antibodies, and analysed by Enhanced Chemiluminescence (ECL, Amersham).

Identification of purified proteins
Proteins were identified either by western blotting with specific antibodies or by microsequencing of internal peptides. The amidoblack-stained bands were excised from the gel and dried under vacuum. They were sent to the Pasteur Institute Protein Sequencing Laboratory (Jacques D'Alayer). The proteins were digested with endolysine C and the generated peptides were separated by HPLC and microsequenced. Sequences were compared with available protein sequences using Blastp (Blast 2.0).

Kinase assays
Kinase activities were assayed in Buffer C at 30°C, at a final ATP concentration of 15 μM. Blank values were subtracted and activities calculated as pmoles of phosphate incorporated for a 10 min incubation and expressed as a percentage of the maximal activity, that is without inhibitors. Controls were performed with appropriate dilutions of Me_2S0. IC_{50} values were estimated from the dose–response curves.

Starfish oocyte CDK1/cyclin B, recombinant mammalian CDK2/cyclin A (provided by W. Harper), CDK5/p25 (kindly provided by J.H. Wang), His-tagged Erk1 and Erk2 (provided by M. Cobb), $p70^{rsk}$ (provided by D. Alessi), CK1 (provided by L. Pinna), were expressed, purified and assayed as described previously [S9].

Supplementary references

S1. Chang, Y.T., *et al.*, & Schultz, P.G. (1999). Synthesis and application of 2,6,9-trisubstituted purine library towards the development of functionally diverse CDK inhibitors. *Chem. Biol.* **6**, 361-375.

S2. Rosania, G.R., Merlie, J., Gray, N., Chang, Y-T., Schultz, P.G. & Heald, R. (1999). A cyclin-dependent kinase inhibitor inducing cancer cell differentiation: biochemical identification using Xenopus egg extracts. *Proc. Natl. Acad. Sci. USA* **96**, 4797-4802.

S3. Borgne, A. & Meijer, L. (1996). Sequential dephosphorylation of $p34^{cdc2}$ on its Thr-14 and Tyr-15 residues at the prophase/metaphase transition. *J. Biol. Chem.* **271**, 27847-27854.

S4. Meijer, L., Azzi, L. & Wang, J.Y.J. (1991). Cyclin B targets $p34^{cdc2}$ for tyrosine phosphorylation. *EMBO J.* **10**, 1545-1554.

S5. Hoessel, R., *et al.*, & Meijer, L. (1999). Indirubin, the active constituent of a Chinese antileukaemia medicine, inhibits cyclin-dependent kinases. *Nat. Cell Biol.* **1**, 60-67.

S6. Walliker, D., *et al.*, and Carter, R. (1987). Genetic analysis of the human malaria parasite *Plasmodium falciparum*. *Science* **236**, 1661.

S7. Zolg, J.W., McLeod, A.J., Dickson, I.H. & Scaife, J.G. (1982). *Plasmodium falciparum*: modifications of the in vitro culture conditions improving parasite yields. *J. Parasitol.* **68**, 1072-1080.

S8. Camargo, E.P. (1964). Growth and differentiation in *Trypanosoma cruzi*: origin of metacyclic trypomastigotes in liquid media. In *Rev. Inst. Med. Trop. Sao Paulo* **6**, 93-100.

S9. Meijer, L., *et al.*, & Moulinoux, J.P. (1997). Biochemical and cellular effects of roscovitine, a potent and selective inhibitor of the cyclin-dependent kinases cdc2, cdk2 & cdk5. *Eur. J. Biochem.* **243**, 527-536.